PREPRINT UCRL-82755

Lawrence Livermore Laboratory

NONDESTRUCTIVE, ENERGY-DISPERSIVE, X-RAY FLUORESCENCE ANALYSIS OF ACTINIDE STREAM CONCENTRATIONS FROM REPROCESSED NUCLEAR FUELS

D. C. Camp and W. D. Ruhter

MASTER

June 27, 1979

This paper was prepared for submittal to the 28th Annual Denver Conference on Applications of X-ray Analysis, University of Denver, July 30 to August 3, 1979

This is a preprint of a paper intended for publication in a journal or proceedings. Since changes may be made before publication, this preprint is made available with the understanding that it will not be cited or reproduced without the permission of the author.

NONDESTRUCTIVE, ENERGY-DISPERSIVE, X-RAY FLUORESCENCE ANALYSIS OF ACTINIDE STREAM CONCENTRATIONS FROM REPROCESSED NUCLEAR FUEL*

D. C. Camp and W. D. Ruhter

Lawrence Livermore Laboratory,
University of California,
Livermore, Calif. 94550

INTRODUCTION

In the event that nuclear fuel from light water reactors (LWR) is reprocessed to reclaim the uranium or plutonium, several analytical techniques will be used for product accountability. Generally, the isotopic content of both the plutonium and uranium in the reprocessed product will have to be accurately determined. One plan for the reprocessing of LWR spent fuel incorporates the following scheme.[1] After separation from both the fission products and transplutonium actinides (including neptunium and americium), part of the uranium and all of the plutonium in a nitrate solution will merge together to form a coprocessed stream. This solution will be concentrated by evaporation and sent to a hold tank for accountability. Input concentrations into the hold tank could be up to 350 g U/ℓ and nearly 50 g Pu/ℓ. The variation to be expected in these concentrations is not known. The remaining uranium fraction will be further purified and sent to a separate storage tank. Its expected stream concentration will be about 60 g U/ℓ. These two relatively high actinide stream concentrations can be monitored rapidly, quantitatively, and nondestructively using the technique of energy-dispersive x-ray fluorescence analysis (XRFA).[2]

*This work was performed under the auspices of the U. S. Department of Energy by Lawrence Livermore Laboratory under contract No. W-7405-Eng-48.

EXPERIMENTAL EQUIPMENT

Excitation Source Requirements

Gamma rays can be used to excite x rays from atoms within a sample. The binding energies of K electrons in U and Pu are 115.59 and 121.72 keV, respectively. Since the primary gamma ray emitted by ^{57}Co has an energy of 122.05 keV, it is an optimum exciting radiation for these two actinide elements. The exciting radiation is usually collimated in some fashion that depends on the geometry of the sample. This is to reduce the amount of radiation that can scatter off of nonsample materials or that can cause them to fluoresce.

Lithium-drifted silicon, Si(Li), is an excellent radiation detector for x rays with less than 30 keV of energy, but it becomes very inefficient for the detection of radiation energies above 60 keV. Since the K x-ray energies of U and Pu extend from 98 to 120 keV, a lithium-drifted or high-purity germanium detector, Ge(Li) or HPGe, is used. For this work a 10-mm-deep, 500-mm^2 HPGe detector was used. It had an energy resolution of 600 eV FWHM for the 122.05-keV gamma-ray peak of ^{57}Co.

The source-detector collimation assembly is shown in Fig. 1. Two ^{57}Co sources are partially collimated to create two beams. The radioactivity was electroplated onto a 1.6-mm-diameter spot and encased in a welded stainless steel capsule* 4.8 mm in diameter and 3.2 mm thick. The 0.37-mm-thick stainless steel plate indicated in Fig. 1 is part of the bottom of the glove box, which was used when handling all of the solutions. The source-detector collimation assembly and liquid-nitrogen (LN) dewar are separate from and located below the glove box. The collimator assembly is 7.5 cm in diameter and 5.0 cm thick.

Since ^{57}Co also emits 570- and 692-keV gamma rays with branching intensities of about 0.16%, as well as other weaker gamma rays above 300 keV, their intensities must be strongly attenuated by introducing shielding between the source and the detector. X rays from lead and Hevimet (tungsten alloy) can also be excited by the source gamma rays; hence, graded absorbers of cadmium and copper are used as liners on the top and bottom surfaces to eliminate these x rays. A central 12.5-mm hole within this collimator assembly allows part of the x rays released within the sample to strike the detector.

*Available from Isotopes Products Laboratories, Burbank, Calif. Reference to a company or product name does not imply approval or recommendation of the product by the University of California or the U.S. Department of Energy to the exclusion of others that may be suitable.

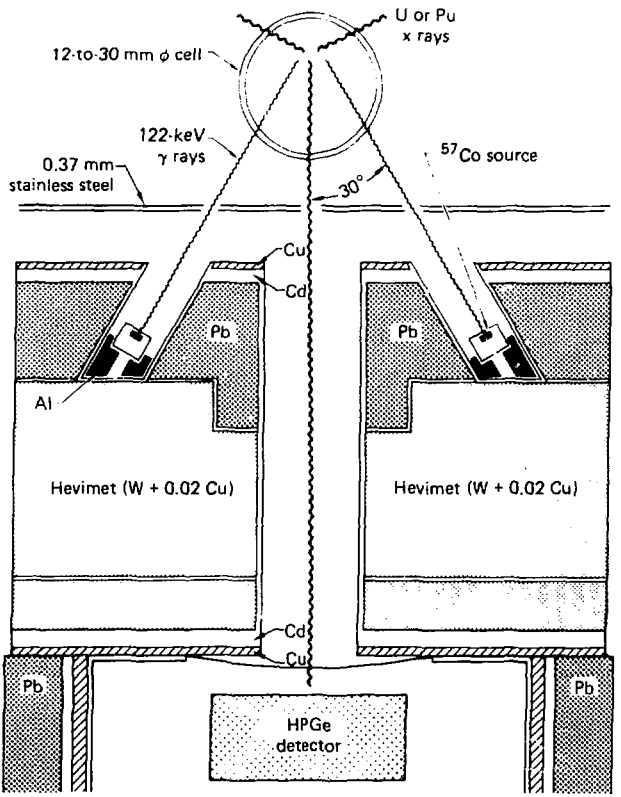

Fig. 1 A cross sectional view of the source exciter and detector collimator assembly. The 0.37-mm stainless steel plate is part of the bottom of a glove box assembly.

In the application of interest here the sample is a solution contained within a cylindrical geometry. A solution cell or pipe section used for calibration purposes could have any diameter, but should be larger than the inside diameter of the detector's collimator. The collimated 122-keV gamma rays interact with atoms in the

solution, creating x rays characteristic of those elements dissolved in the solution. A portion of the emitted x rays are collimated to strike the detector, and from the energies and intensities detected the elemental concentrations in the solution can be determined.

The HPGe detector cryostat used in these experiments utilized a beryllium window, but such a window is not necessary if actinide K x rays are to be detected. Clearly, the x-ray intensity recorded by the HPGe detector increases as the sample volume-to-detector distance decreases. However, this distance cannot be decreased indefinitely. As the distance is decreased, less shielding is possible between the intense ^{57}Co sources and the detector. Those higher energy gamma rays, which pass through the Hevimet and interact with the HPGe detector, create a Compton continuum that appears as a constant, energy independent background in the vicinity of U and Pu x rays. This background contribution increases very rapidly with decreasing amounts of shielding, degrading the x-ray signal-to-noise ratio quickly. Some high Z shielding is also required around the detector housing (above the cryostat) to reduce background radiation detected from the local environment and source-air scattering.

The radiation sources and detector collimator are necessarily coupled to the detector and its LN dewar, which was located below the glove box containing the solution cell. A glove box must be used when handling solutions containing Pu so that, in the event of a spill, contamination is confined.

Solution Cells

In an actual reprocessing plant, U and Pu solutions will probably flow through stainless steel pipes. In order to examine the behavior of these solutions when in motion, a flow system was constructed. A variable speed peristaltic pump moves the solution through the Tygon tubing and cell by a cyclical squeezing action. The solution circulates from the separatory funnel through the cell and pump, and then is returned to the funnel. The flow direction can be reversed if desired.

Calibrated, unknown, or wash nitric acid solutions containing only U were transferred from their containers to the separatory funnel by use of a unidirectional air flow hand pump. This avoided any pouring action. Quantitative transfers were usually not necessary. By reversing the dual-channel stopcock, one could empty the flow system using the peristaltic pump. Since 2 to 3% of the solution remained in the tubing, the system was flushed out after each use, and then primed with a solution close in concentration to the next to be measured. The glass cell allowed visual inspection of the flow conditions. Three sizes of Pyrex cells, 12, 25, and 38 mm in outside diameter, were used.

Once it was demonstrated that the x-ray intensities were independent of whether the solution was flowing or static, solution cells were constructed using stainless steel (SS). Each cell was machined to have an outside diameter of 18.80 mm and 1.50-mm-thick walls. They had a nominal solution length of 10.0 cm. SS cells filled with Pu nitrate or mixed U-Pu nitrate had to be handled in a sealed glove box environment. To insure repeatability in the measurements, both the Pyrex cells and SS cells could be positively located in a reproducible position with respect to the detector collimation axis.

Computer-Based Analyzer

The x rays released in the solution samples were detected by the HPGe detector. Preamplified pulses were routed to a Canberra 1413 amplifier and 1468A pile-up rejector. Valid output pulses were routed to a Nuclear Data ND600 pulse height analyzer (PHA). The PHA, with its own LSI-11 microprocessor, was coupled to an LSI-11 minicomputer that had a 32K 16-bit-word memory. A dual floppy disk was coupled to the LSI-11 and each disk had a 216K-byte (108K-word) capacity. Also, a dual hard disk system with a 10M-byte capacity was coupled to the LSI-11. Other system peripherals include a Hazeltine video teletypewriter terminal, an LA-180 high-speed line printer, and a Tektronix digital data plotter.

A computer-based pulse height analyzer added a considerable amount of versatility to the experimental system. In fact, in an actual reprocessing installation a computer-based data analysis system would be essential, and probably would be linked to a command computer center. This particular system allowed successive spectra to be stored on disk and permitted spectrum analysis to be carried out simultaneously while data were also being acquired. Whatever automatic analysis sequence is desired, appropriate software can be written and stored on floppy disk. Generally, the software programs can be written in FORTRAN, BASIC or another language familiar to the user.

EXPERIMENTAL PROCEDURES AND RESULTS

Spectra

The spectrum shown in Fig. 2 is the result of an x-ray fluorescence analysis of pure uranium nitrate solution at 100 g U/ℓ contained in a 25-mm-diameter cylindrical Pyrex cell. Total analysis time was 334 live time seconds at 19.4% analyzer dead time, using two 5-mCi ^{57}Co sources. The net Kα1 x-ray intensity is almost 2×10^5 counts. The energy region shown extends from 0 to 200 keV. One of the more dominant features in the spectrum is the broad, intense peak centered at about channel 450. This peak is a result of the primary exciting radiation (the 122-keV gamma ray of ^{57}Co) incoherently (Compton) scattering through an angle of 140°.

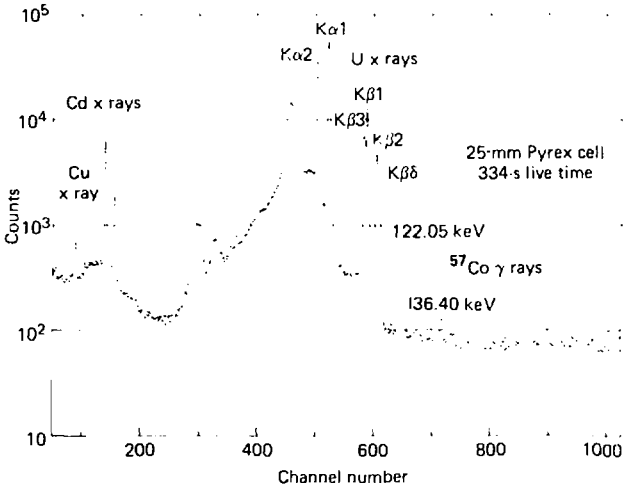

Fig. 2 A 1024-channel XFRA spectrum of 100-g-U/ℓ uranium nitrate in the 25-mm cell. The cadmium x rays result from a liner on the inner wall of the detector collimator. The two broad peaks above channel 300 are incoherently scattered platinum (source backing material) x rays.

The sharp, intense peaks located between channels 500 and 620 are the K x rays of U. The most intense x ray is Kα1 at 98.439 keV. Kα2 is about half as intense and located slightly lower in energy at 94.665 keV. The Kβ x rays contain more than one component. Hence, they appear as multiplets. The (Kβ1 + Kβ3 + Kβ5) x ray is located near channel 584, while (Kβ2 + Kβ4 + Kδ) is less intense and is located near channel 608. The weak 122-keV peak at about channel 644 is coherently scattered (no energy change) exciting radiation. The very weak peak observed at channel 720 is coherently scattered 136.4-keV gamma ray also from ^{57}Co. Its intensity is one-tenth that of the 122-keV radiation. The short, nearly flat distribution centered about channel 488 is the 140° incoherently scattered radiation from the 136.4-keV gamma ray.

Figure 3 shows an expanded view of a fluorescence spectrum of the 80- to 130-keV region for two different concentrations of U in nitric acid. The most intense spectrum represents a concentration

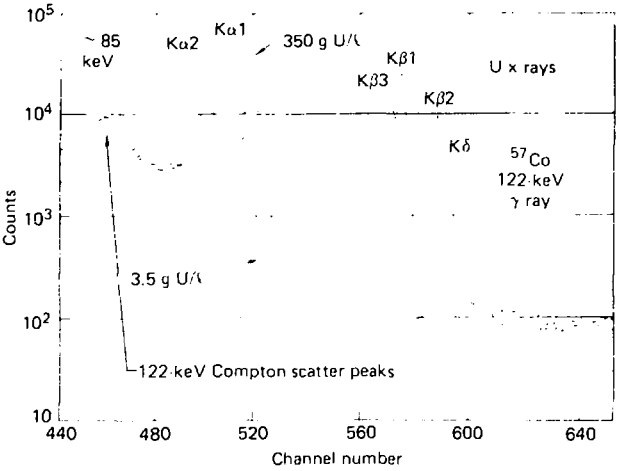

Fig. 3 Two spectra of uranium x rays in the 80-to-130-keV region for two concentrations of uranium nitrate plotted for equivalent counting times. Note the behavior of the incoherent and coherent scattering peaks of the 122-keV exciting radiation versus concentration.

of 350 g U/ℓ; while the weaker spectrum results from a nitrate solution containing only 3.5 g U/ℓ. These two spectra span a dynamic concentration range of 100. The actual dynamic range offered by the XRFA technique is in excess of 1000; however, it is most useful for concentrations above 1 g U/ℓ. Below 1 g U/ℓ the counting times required become much longer in order to obtain sufficient statistical accuracy.

Note that as the solution concentration increases the intensity of the coherently scattered exciting radiation peak at 122 keV increases (because the effective Z of the solution increases). Also, as the solution concentration increases, the broad incoherently scattered 122-keV peak at about 85 keV decreases in intensity and shifts slightly toward a higher energy. The increase in energy of this peak from 3.5 g U/ℓ to 350 g U/ℓ is 0.79 keV, which corresponds to a change from 143.6° to 138.7° in the backscattering angle. In effect, at higher concentrations the center of the solution volume

exposed moves slightly closer to the detector, thus decreasing the backscattering angle.

The top spectrum in Fig. 4 shows an expanded view of the 80- to 130-keV spectrum region for U and Pu nitrate solution. The U concentration is 350 g U/ℓ; while the Pu concentration is 48 g Pu/ℓ. This

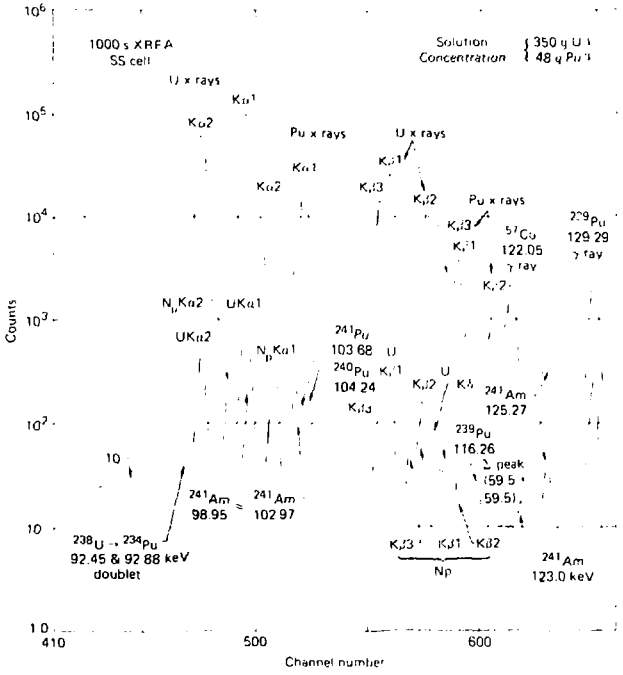

Fig. 4 The top spectrum is an XRFA of a mixed uranium plutonium nitrate solution in a stainless steel cell. Their respective concentrations are shown. The lower spectrum results from the natural radioactivity in the solution. It is plotted one decade lower for clarity: the 129.29-keV peak from ^{239}Pu in the top spectrum results entirely from the solution's natural radioactivity.

mixture corresponds closely to the U-Pu concentration ratio expected to flow into the final hold tank from a nonspiked, coprocessed product stream. The principal features in this spectrum are the fluoresced x rays of U and Pu and several Pu gamma rays from its natural radioactivity. The natural radioactivity arising from this U-Pu solution is shown in the lower spectrum, which has been plotted one decade lower for clarity. All features in the spectrum have been identified; however, many of these are quite different than those expected in the XRFA of a freshly reprocessed nitrate stream. These differences merit some discussion.

The difference in isotope percentages will have the following influence on the natural radioactivity issuing from a freshly reprocessed U-Pu nitrate stream. The 92.45- and 92.88-keV doublet gamma ray in ^{234}U from the decay of ^{238}U will still be present, but will not be significantly troublesome. The neptunium K x-ray intensity, which accompanies the decay of ^{237}U and ^{241}Am, should be less intense. The ^{241}Am, which has been chemically separated, will not have its 98.95-, 102.97-, 123.0-, and 125.29-keV gamma rays present. The (59.53 + 59.53-keV) sum peak at 119.06 keV will be absent. The ^{241}Pu 103.68-keV gamma ray will be much stronger. The ^{240}Pu 104.24-keV gamma ray will also be stronger. The ^{239}Pu gamma-ray lines at 98.71, 116.26, 124.5, and 129.29 keV will not be as strong.

Finally, it is difficult to say how strong the U K x-ray lines will be from natural radioactivity. They will grow in strength as the α-decay of ^{241}Pu approaches equilibrium, after about 42 d. A small contribution from internal α and γ self-fluorescence may be present but will depend on solution concentration. Any separated ^{237}U blended back into the coprocessed stream will contribute to the neptunium K x-ray intensity. Since the Pu isotope percentages will not remain the same from fuel batch to batch, the natural radioactivity in the coprocessed stream will have to be monitored. Thus, it appears that in the x-ray spectrum U Kα1 and Pu Kα2 will be relatively free of interference, but Pu Kα1 will have strong contributions from the ^{240}Pu, 104.24-keV and the ^{241}Pu, 103.68-keV gamma rays.

Count Rate vs Concentration and Cell Calibration

A set of standard solutions were prepared using ACS-grade natural uranium nitrate. Sufficient HNO_3 acid was used to adjust the acid concentration to 3.0M. The standards covered the range from 0.6 g U/ℓ to 350 g U/ℓ and their values were determined by potential coulometry. The solutions were introduced into the flow system as described earlier. The 25-mm-diameter Pyrex cell was the first to be used, and Fig. 4 showed a spectrum obtained from the 100-g-U/ℓ solution. Generally, to obtain data for each concentration three separate runs were made with the system under flow (or static) conditions once or twice out of the three runs. Analysis live times

for each run were set to obtain better than 0.5% statistics (40,000 counts) in the gross Kα1 peak, but no run was less than 100 s. Only one long run was used to obtain data on solution concentrations ≤ 1 g U/ℓ. Subsequently, this procedure was repeated for the 12-mm Pyrex cell. For the 38-mm Pyrex cell and SS cell, data were obtained with the solution not flowing. Other extensive experiments had confirmed that concentration measurements made on the solution under either flow or static conditions were equivalent (see the next section).

Figure 5 shows the net counting rate in counts/s (left border) for the U Kα1 peak as a function of solution concentration (top border), as measured with the 25-mm Pyrex cell. The two similarly

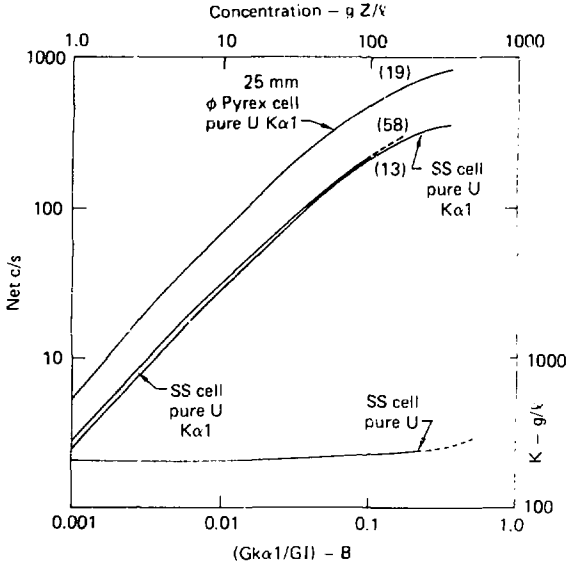

Fig. 5 A log-log plot of the measured net count rate (left) versus solution concentration (top) for single element solutions in the Pyrex and stainless steel cells. The lower curve shows the behavior of the calibration constant K (right) versus the experimentally determined ratio (bottom).

shaped curves below this give the count rate observed for Pu Kα1 or U Kα1 for unmixed solutions of plutonium or uranium nitrate respectively, in the SS cell. The small figures in parentheses indicate the analyzer dead times in percent for 100-g/ℓ solution concentrations in each cell type. The Pu solution contained natural radioactivity. The U solution in the SS cell contained less solution volume than the 25-mm Pyrex cell, hence its lower dead time.

As the solution concentration is increased, there is less than a linear increase in the count rate. This decline in count rate is a combination of increasing self-absorption of the Kα1 x ray within the solution and an effective decrease in the solution volume as the concentration is increased. Clearly, the net count rate observed will depend on the ^{57}Co source strength ($T_{1/2}$ = 270 d), the experimental geometry and cell wall thickness, and the HPGe detector efficiency. Such a simple curve showing count rate vs concentration is not time independent. Furthermore, at high concentrations the rate of change of count rate with concentration becomes less sensitive (i.e., a 1% change in count rate corresponds to a 4% change in concentration at 300 g U/ℓ for the 25-mm cell). The observed count rate is also sensitive to minor changes in geometry and system dead time, which varies with concentration. Air bubbles in a flowing stream would also affect the observed count rate. So, it is desirable to define a calibration procedure which is independent of source half-life and system dead time, insensitive to minor changes in geometry and stream flow conditions, and more sensitive to concentration changes.

It can be seen from the two spectra in Fig. 3 that as the x-ray intensity increases, the 140°, incoherently scattered, 122-keV radiation at 86 keV decreases. The ratio of the Kα1 x-ray intensity to a portion of the spectrum that includes the incoherent peak is almost independent of concentration. The concentration in g/ℓ can be related to this ratio by the formula

$$C = K\left[\frac{GK\alpha 1}{GI} - B\right] \qquad (1)$$

where GKα1 is the gross count within a window including the Kα1 x-ray peak, GI is the gross count in a window including the incoherent peak, and K is a nonlinear calibration parameter in g/ℓ. The constant B is the ratio GKα1/GI for pure nitric acid. This ratio is independent of source exciter half-life, changes in dead time, and small changes in geometry. Thus, the bracketed quantity in Eq. (1) is an experimentally measured quantity. If a well-defined relationship between K and the bracketed quantity can be established, then their product will yield the concentration.

The lower portion of Fig. 5 shows the behavior of K (right border) vs this ratio (lower border) for the SS cell containing pure uranium nitrate solution. The increase in K at higher concentrations is effectively a result of increasing self-absorption of U Kα1 and decreasing fluoresced volume as the solution concentration increases. A least squares fit to K, expressed as a polynomial function of the natural logarithm of the bracketed quantity, results in the equation shown as an inset at the top of Fig. 6. This figure shows the percentage deviation between the calculated and experimental K as a function of solution concentration in the SS cell. The mean absolute value difference is 0.34% with a root mean square deviation of 0.20%.

Dynamic Concentration Measurements

One of the advantages of the Pyrex cell (coupled to the peristaltic pump via Tygon tubing) is the ability to observe the solution under flow or static conditions while a measurement is in progress. The ND-600 disk-based analyzer system was programmed to carry out an analysis for a preset time Δt s, store the results on disk, clear the memory, and begin a new analysis, again for Δt s. Data transfer and memory clearance required a minimum of 10 s. This cycle could be repeated n times, where n was a preselected integer. Data could be taken in this manner with the solution either static or flowing.

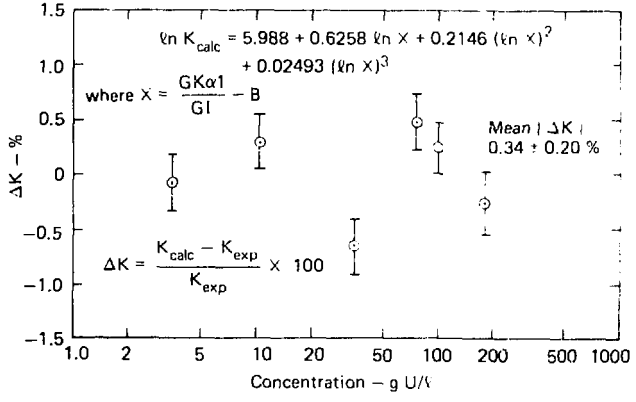

Fig. 6 A semilog plot for the residuals ΔK versus the concentration. The equation used to calculate K is shown. The mean |ΔK| is 0.34 ± 0.20%.

The top section of Fig. 7 shows a set of 24 measurements; however, the first and last six measurements were made with the solution static, while the central 12 measurements were made with the solution flowing at 80 &/h. The static and flow results overlap well within the precision of their standard errors, which are slightly larger (0.70%) than for the 24-cycle static run (0.65%).

Another advantage of the flow system is the ability to demonstrate dynamic concentration measurements. By introducing a known volume into a dry cell and tubing system, small volumes of pure 3.0M HNO_3 acid can be introduced into the separatory funnel. These volumes are such as to lower the concentration by known small increments. Similarly, by introducing known volumes of a more concentrated solution, the concentration can be increased. In this manner concentration changes in an actual flowing stream can be simulated. The lower section of Fig. 7 illustrates such measurements. Initially, 100.0 ml of the 100.0-g-U/& standard solution was introduced

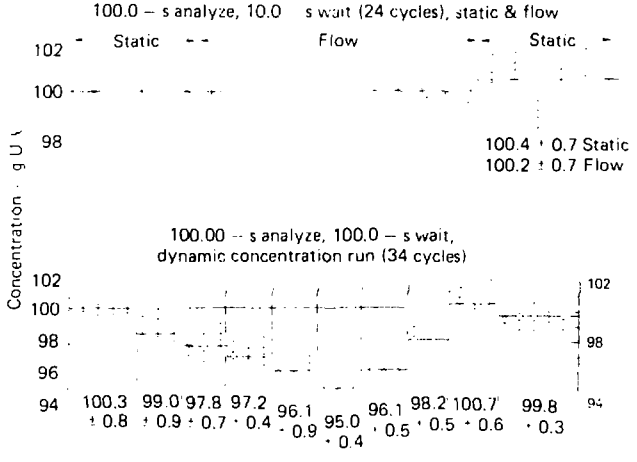

Fig. 7 Two plots of solution concentration versus time. Analysis time and pause times vary. The top set of data points was taken with the first and last six measurements static, and the center 12 measurements flowing; the lower set is a dynamic concentration run (see text). The error bars indicate 1σ statistical counting accuracy only.

into the flow system with the cell out of the flow. Appropriate volumes of pure 3M HNO_3 were calculated and metered out so that they could be introduced into the flow system. This caused a concentration reduction of exactly 1.0 g U/ℓ for each of five times. Then, appropriate volumes of more concentrated uranyl nitrate solutions were introduced, to increase the entire solution volume 2.0 g U/ℓ for each of three steps. This returned the system to 101 g U/ℓ, whereupon a final calculated volumetric addition of pure 3M HNO_3 returned the solution to its original 100.0-g-U/ℓ concentration.

The pause time of 100 s was selected on the basis of earlier dynamic concentration runs. It was somewhat longer than the time required for the solution volume to reach equilibrium after introduction of an additional volume. Again each 100-sample analysis had approximately the same statistical accuracy of 0.2%; however, the mean values indicated for each successive concentration change are determined from just the measurements made within each interval. Unfortunately for the seventh concentration change (to 94 g U/ℓ), the data storage disk filled up and the system went off. After the next concentration adjustment, data storage was continued on a new disk. Note that the mean of the first and last five system concentrations is 100.05 ± 0.62 g U/ℓ, in excellent agreement with the mean value of 100.13 ± 0.40 g U/ℓ from the first to last flow cycle measurements.

REFERENCES

1. T. J. Warren, W. E. Prout, M. C. Thompson, M. J. [illegible], and G. S. Nichols, Technical Data Summary Concerning a Solvent Extraction Facility, Savannah River Laboratory, Document DPSTD-AFCT-77-9 (December, 1977).
2. D. C. Camp, An Introduction to Energy Dispersive X-Ray Fluorescence Analysis, Lawrence Livermore Laboratory, Livermore, California, UCRL-52089 (June, 1978).